

Stabilizing strongly correlated photon fluids with a non-Markovian reservoir

José Lebreuilly,^{1,*} Alberto Biella,^{2,3} Florent Storme,²

Davide Rossini,^{4,3} Rosario Fazio,^{5,3} Cristiano Ciuti,² and Iacopo Carusotto¹

¹*INO-CNR BEC Center and Dipartimento di Fisica, Università di Trento, I-38123 Povo, Italy*

²*Université Paris Diderot, Sorbonne Paris Cité, Laboratoire Matériaux et Phénomènes Quantiques, CNRS-UMR 7162, 75013 Paris, France*

³*NEST, Scuola Normale Superiore & Istituto Nanoscienze-CNR, I-56126 Pisa, Italy*

⁴*Dipartimento di Fisica, Università di Pisa and INFN, Largo Pontecorvo 3, I-56127 Pisa, Italy*

⁵*ICTP, Strada Costiera 11, 34151 Trieste, Italy*

We explore the physics of strongly correlated photons in arrays of coupled nonlinear resonators in presence of a novel frequency-dependent incoherent pump scheme with a square-shaped spectrum, which we propose to implement via a reservoir of population-inverted two-level emitters with a broad distribution of transition frequencies. The scheme is predicted to stabilize a non-equilibrium steady state sharing important features with a zero-temperature equilibrium state with a tunable chemical potential. We confirm this for the Bose-Hubbard model by computing numerically the steady state for finite system sizes: first, we predict the existence of an incompressible Mott-Insulator-like state, which is robust against tunneling and losses, with an arbitrary integer density. Secondly for non-integer densities or stronger tunneling, the system enters a coherent regime analogous to the superfluid state. Specific features related to the non-equilibrium nature of the steady state are pointed out.

Introduction. Over the last decade, technological developments in optical devices have allowed to engineer materials presenting strong photon-photon interactions [1–3], and a growing interest has been devoted to the possibility of stabilizing strongly correlated photonic gases. The so-called photon blockade regime [4], in which photons behave as impenetrable particles, has been reached in various single-mode cavity platforms embedding atoms [5], superconducting qubits [6], or quantum dots [7, 8], as well as in Rydberg EIT atomic gases [9, 10]. However, even though non- [11–13] or weakly-interacting gases [14–16] have been widely studied in extended systems, scaling up strong non-linearities into large lattices still remains an open challenge [17].

Overcoming such an obstacle would be an essential step toward the stabilization of novel photonic phases [18–20], including Fractional Quantum Hall states [21, 22], as well as the Mott Insulator (MI) [23, 24] in which the photon blockade prevents the onset of extended coherence. In particular, the latter state has been predicted for isolated equilibrium photonic Bose-Hubbard (BH) [25] and Jaynes-Cummings-Hubbard [26, 27] models, under the requirements of an integer photon density and low enough temperatures. In order to apply these results to photonic systems, one has to keep in mind that the particle number is hardly conserved in realistic set-ups and heating effects cannot be neglected. It is thus essential to develop general schemes to tame and possibly exploit the intrinsic non-equilibrium nature of photonic systems.

While, up to now, most studies focused on how to use a coherent drive to refill the photonic population [28–31], a couple of recent works [2, 22] have proposed to employ frequency-dependent incoherent pumps in order to avoid coherent re-absorption processes. However, the Lorentzian spectrum considered there did not allow to target selectively the transitions, and the resulting Mott state was not robust against tunneling [2]. Other studies have proposed to use a parametric coupling to a thermal bath of excitations in order to generate an artificial chemical potential [33], or to cool down a coher-

ently driven photonic system by using frequency-dependent losses [34], in analogy with evaporative cooling in cold-atom systems [35].

In this Letter, we propose a simple yet realistic implementation of a non-Markovian incoherent pump with a tailored emission spectrum by using population-inverted two-level emitters with a broad distribution of transition frequencies. We then show how a square-like emission spectrum allows to cool strongly correlated photonic systems toward ground-state-like steady states with a tunable effective chemical potential. We illustrate our proposal on the paradigmatic case of a one-dimensional (1D) BH model and we numerically show how it is possible to stabilize Mott-Insulator-like states with an arbitrary integer photon density which are robust against tunneling and losses. For non-integer densities or higher tunneling, our finite-size system exhibits a crossover towards a coherent state reminiscent of the superfluid to Mott insulator transition of equilibrium systems.

The Model. We consider a driven-dissipative model for photons in an array of L coupled nonlinear cavities:

$$H_{\text{ph}} = \sum_{i=1}^L \left[\omega_{\text{cav}} a_i^\dagger a_i + \frac{U}{2} a_i^\dagger a_i^\dagger a_i a_i \right] - \sum_{\langle i,j \rangle} J a_i^\dagger a_j, \quad (1)$$

where a_i (a_i^\dagger) are bosonic annihilation (creation) operators for photons in the i -th cavity. We focus on the weakly-dissipative regime, in which photonic losses and emission processes are slow with respect to the bath memory time scales. The density matrix ρ obeys the following Redfield master equation [1] ($\hbar = 1$):

$$\partial_t \rho(t) = -i [H_{\text{ph}}, \rho(t)] + \mathcal{L}_1[\rho(t)] + \mathcal{L}_{\text{em}}[\rho(t)], \quad (2)$$

with $[\cdot, \cdot]$ being the commutator. Markovian losses are modeled by a usual Lindblad term $\mathcal{L}_1[\rho] = \frac{\Gamma_1}{2} \sum_{i=1}^L \mathcal{D}[a_i; \rho]$ with $\mathcal{D}[\mathcal{O}; \rho] = 2\mathcal{O}\rho\mathcal{O}^\dagger - \mathcal{O}^\dagger\mathcal{O}\rho - \rho\mathcal{O}^\dagger\mathcal{O}$. The key novelty of this work is to use a frequency-dependent incoherent pump,

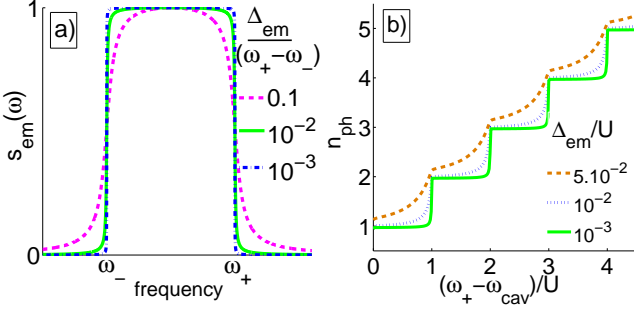


FIG. 1: Panel a): Reservoir emission spectrum $s_{\text{em}}(\omega)$ for various values of Δ_{em} . Panel b): Average photon number n_{ph} for a 1 site system as a function of $\mu = \omega_+ - \omega_{\text{cav}}$ (varying ω_{cav}) for various values of Δ_{em} . Parameters of the right panel: $\Gamma_{\text{em}}^0/U = 3 \cdot 10^{-4}$, $\Gamma_1/U = 10^{-5}$, $\omega_-/U = -40$.

so that the emission term

$$\mathcal{L}_{\text{em}}(\rho) = \frac{\Gamma_{\text{em}}^0}{2} \sum_{i=1}^k \left[\tilde{a}_i^\dagger \rho a_i + a_i^\dagger \rho \tilde{a}_i - a_i \tilde{a}_i^\dagger \rho - \rho \tilde{a}_i a_i^\dagger \right] \quad (3)$$

does not have a standard Lindblad form and involves modified lowering (\tilde{a}_i) and raising (\tilde{a}_i^\dagger) operators:

$$\frac{\Gamma_{\text{em}}^0}{2} \tilde{a}_i = \int_0^\infty d\tau \Gamma_{\text{em}}(\tau) a_i(-\tau). \quad (4)$$

Here, the kernel $\Gamma_{\text{em}}(\tau) = \theta(\tau) \int \frac{d\omega}{2\pi} \mathcal{S}_{\text{em}}(\omega) e^{-i\omega\tau}$ takes into account the reservoir emission spectrum $\mathcal{S}_{\text{em}}(\omega)$, while the $a_i(t)$ operators are defined in the interaction picture with respect to the photonic Hamiltonian, $a_i(\tau) = e^{iH_{\text{ph}}\tau} a_i e^{-iH_{\text{ph}}\tau}$. Thus, considering two eigenstates $|f\rangle$ (resp. $|f'\rangle$) of the photonic Hamiltonian with N (resp. $N+1$) photons and energy ω_f (resp. $\omega_{f'}$), the matrix element of the modified jump operators equals

$$\langle f | \tilde{a} | f' \rangle = \frac{2}{\Gamma_{\text{em}}^0} \Gamma_{\text{em}}(\omega_{f'f}) \langle f | a | f' \rangle, \quad (5)$$

with $\omega_{f'f} = \omega_{f'} - \omega_f$ and $\Gamma_{\text{em}}(\omega) = \frac{1}{2} \mathcal{S}_{\text{em}}(\omega) - i\delta_l(\omega)$. The imaginary part of $\Gamma_{\text{em}}(\omega)$ gives rise to a rather small Lamb-shift $\delta_l(\omega)$ compared to the emission linewidth (see Supplemental Material [37]), and thus does not bring important physical effects. In contrast, the real part $\mathcal{S}_{\text{em}}(\omega)/2$ is physically essential as it provides the frequency-dependent emission rate.

The physics and the phase diagram of this driven-dissipative model critically depend on the specific choice of the emission spectrum. In contrast with our previous work [2] in which the emission spectrum was Lorentzian, we will focus here on the study of a “square-shaped” spectrum $\mathcal{S}_{\text{em}}(\omega) = s_{\text{em}}(\omega) \Gamma_{\text{em}}^0$, shown in Fig. 1 a), which maintains an almost constant value Γ_{em}^0 all over a frequency domain $[\omega_-, \omega_+]$, and decays smoothly with a power law outside this interval over a frequency scale $\Delta_{\text{em}} \ll \omega_+ - \omega_-$. While the lower cutoff can be set to a very far red-detuned frequency, $(\omega_{\text{cav}} - \omega_-) \gg U, J \geq 0$, the key role is played

by the upper cutoff ω_+ . The weak dissipation condition reads: $\Gamma_1, \Gamma_{\text{em}}^0 \ll \Delta_{\text{em}}, (\omega_+ - \omega_-)$.

Experimental proposal. To engineer the above pump, we propose to insert a set of $N_{\text{at}} \gg 1$ two-level atoms/emitters into each cavity according to the Hamiltonian $H_{\text{at}} + H_I = \sum_{i=1}^k \sum_{n=1}^{N_{\text{at}}} [\omega_{\text{at}}^{(n)} \sigma_i^{+(n)} \sigma_i^{-(n)} + \Omega_R (a_i^\dagger \sigma_i^{-(n)} + \text{h.c.})]$, where $\sigma_i^{-(n)}$ ($\sigma_i^{+(n)}$) are the lowering (raising) operators for the two-level n -th atom in the i -th cavity and Ω_R is the single-atom Rabi frequency. The transition frequencies $\omega_{\text{at}}^{(n)}$ of the different emitters are assumed uniformly distributed over the interval $[\omega_-, \omega_+]$.

Each atom is incoherently pumped in the excited state at a rate Γ_p , which is modeled by the Lindblad term $\mathcal{L}_{p,\text{at}}[\rho_{\text{tot}}] = \frac{\Gamma_p}{2} \sum_{i=1}^k \sum_{n=1}^{N_{\text{at}}} \mathcal{D}[\sigma_i^{+(n)}; \rho_{\text{tot}}]$. The total {cavity+atoms} density matrix ρ_{tot} obeys the master equation:

$$\begin{aligned} \frac{d}{dt} \rho_{\text{tot}}(t) = & -i [H_{\text{ph}} + H_{\text{at}} + H_I, \rho_{\text{tot}}(t)] \\ & + \mathcal{L}_l[\rho_{\text{tot}}(t)] + \mathcal{L}_{p,\text{at}}[\rho_{\text{tot}}(t)], \end{aligned} \quad (6)$$

The atomic pump induces an almost perfect inversion of population: atoms undergo irreversible cycles in which they de-excite by emitting a photon in the cavity and are immediately re-pumped so to avoid reabsorption.

Due to the broadening induced by the pump, each atom displays an Lorentzian emission spectrum of linewidth Γ_p ; integration over the broad emitter distribution yields the desired square shaped spectrum. Under the constraints $\sqrt{N_{\text{at}}} \Omega_R, \Gamma_1 \ll \Gamma_p$, we can use projective methods [1] to trace out the atomic degrees of freedom [2, 37] and write a closed master equation for the photonic density matrix in the form of Eq. (S19) with $\mathcal{S}_{\text{em}}(\omega)$ given by Fig. 1 a), with $\Delta_{\text{em}} = \Gamma_p$. For $\Gamma_p = \Delta_{\text{em}} \ll \omega_+ - \omega_-$, we obtain $\Gamma_{\text{em}}^0 = 2\pi N_{\text{at}} \Omega_R^2 / (\omega_+ - \omega_-)$.

Steady-state equilibrium-like properties. In a single cavity geometry, this allows to stabilize pure Fock states with arbitrary photon number: indeed, in Fig. 1 b) we observe a plateau structure with successive jumps between integer values of the steady-state photon number, with a smooth (resp. sharp and discontinuous) transition for $\Delta_{\text{em}}/U \gtrsim 1$ (resp. $\Delta_{\text{em}}/U \ll 1$) between the various steps. The physical quantity $\omega_+ - \omega_{\text{cav}}$ manifestly plays a similar role as the chemical potential in equilibrium physics [23] but with a mechanism differing from [33].

Pushing the analogy with equilibrium forward, we find that the specific shape of the pump spectrum [Fig. 1 a)] allows to overcome the fragility against tunneling pointed out in [2] for Lorentzian pumps, so to drive large many-cavity systems toward a steady state closely related to a $T = 0$ state. To see this, let us set a strong emission at resonance $\Gamma_{\text{em}}^0 \gg \Gamma_1$, while maintaining a sharp cut-off at the edges of the spectrum $\Delta_{\text{em}} \ll U$, in such a way to strongly favor (resp. block) $f \rightarrow f'$ transitions verifying $\omega_{f'f} \leq \omega_+$ (resp. $\omega_{f'f} \geq \omega_+$). Under those constraints, the transition rates follow the condition

$$\frac{\mathcal{T}_{f \rightarrow f'}}{\mathcal{T}_{f' \rightarrow f}} \simeq \frac{\Gamma_{\text{em}}^0}{\Gamma_1} \theta(\omega_+ - \omega_{f'f}) \quad \left\{ \begin{array}{ll} \gg 1 & \text{if } \omega_{f'f} < \omega_+ \\ \ll 1 & \text{if } \omega_{f'f} > \omega_+ \end{array} \right.,$$

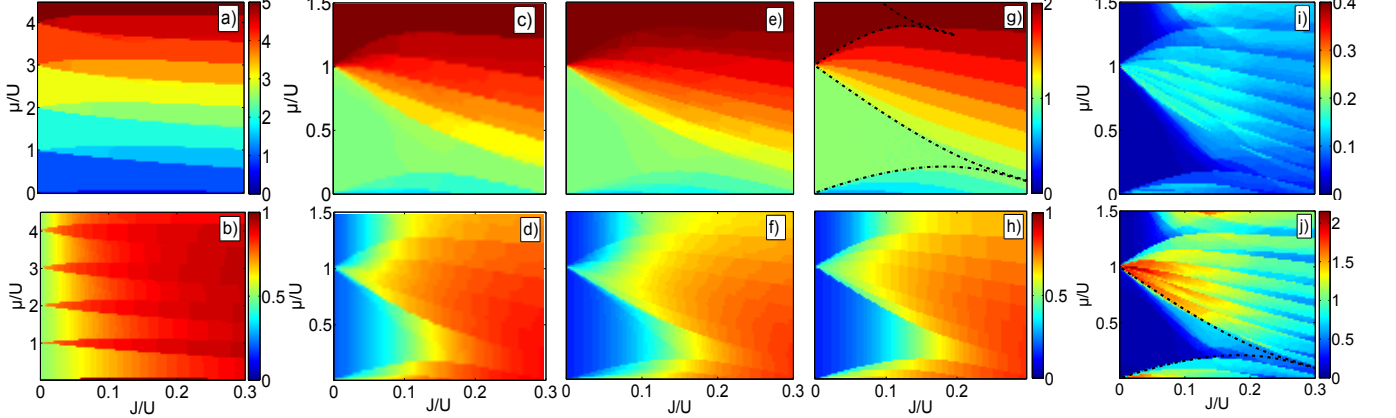


FIG. 2: Steady-state properties for a limit choice of parameters. Panels a),c),e) [resp. panels b),d),f)] Average steady-state photon number per site n_{ph} (resp. condensed fraction x_{BEC}), for $L = 2, 5, 7$ respectively. Panel g) [resp. panel h): Average n_{ph} (resp. x_{BEC}) in a $T = 0$ equilibrium system, for $L = 7$. Panel i) [resp. panel j): steady-state particle number relative fluctuations ΔN [resp. entropy $S = \langle \ln(\rho_{\infty}) \rangle$], for $L = 7$. In panel g) and j) dash dotted black lines indicate the MPS $T = 0$ prediction for the first Mott lobes. Parameters used in all panels (except g,h): $\Gamma_1/\Gamma_{\text{em}}^0 = 10^{-3}$, $U/\Delta_{\text{em}} = 10^6$, $\Gamma_{\text{em}}^0/\Delta_{\text{em}} = 10^{-2}$, $\omega_+ = 0$, $\omega_-/\Delta_{\text{em}} = -4 \times 10^7$. Cutoff in particle number per site $N_{\text{max}} = 6$ [Panels a),b)] and $N_{\text{max}} = 3$ [panels c)-j)]

that closely resembles a $T = 0$ detailed-balance relation: $(T_{f' \rightarrow f}/T_{f \rightarrow f'})_{\text{eq}} = e^{\beta(\omega_+ - \omega_{f'f})}$ with $\beta \rightarrow +\infty$. One may thus expect the many-body steady state to be very close to the ground state $|\text{GS}\rangle$ of the rotating frame Hamiltonian $H_{\text{eff}} = H_{\text{ph}} - \omega_+ N$, i.e., a $T = 0$ state with chemical potential $\mu = \omega_{\text{cav}} - \omega_+$.

Numerical results for finite periodic chains. For system sizes going up to $L = 5$ sites, we employed an exact numerical calculation of the steady-state density matrix $\rho_{\infty} \equiv \rho(t \rightarrow +\infty)$ of Eq. (S19). Above 5 sites, the secular approximation [43] was adopted. This approximation, which holds for weak dissipation but can be problematic in the presence of degeneracies, has been verified for our choice of parameters to give indistinguishable results from the exact solution for small systems sizes [44]. To facilitate the readers, we start our discussion from a limit case of parameters for which the physics is most transparent [Fig. 2], and then will move as a second step toward experimental state-of-the-art parameters in order to assess the robustness of the various features [Fig. 3].

The steady-state photon density $n_{\text{ph}} = \langle N \rangle / L$ and the Bose-condensed fraction $x_{\text{BEC}} = \langle n_{k=0} \rangle / \langle N \rangle$ (where $\langle O \rangle \equiv \text{Tr}(O\rho_{\infty})$) are given in Fig. 2 [panels a)-f)] for several system sizes L , and are compared to the $T = 0$ equilibrium predictions for $L = 7$ sites [panels g), h)]. Even though one does not expect a true BEC for an infinite 1D chain [38], still x_{BEC} provides physical insight on the long-range coherence properties of our finite-size system. Extending our study to higher dimensions requires more sophisticated numerical methods [45] and will be the subject of a forthcoming work [39].

Apart from the presence of small corrections that will be discussed below, the qualitative agreement between the observables calculated for the driven-dissipative steady state and the $T = 0$ prediction of the equilibrium BH model is very good: first, we observe for increasing μ a series of insulating-like regions with successive integer values of the density n_{ph}

and a small x_{BEC} . In this regime, the photonic density does not depend on the Hamiltonian parameters ω_{cav} and J , and there are almost no fluctuations in the total photon number since $\Delta N \equiv \sqrt{\langle N^2 \rangle - \langle N \rangle^2} / \langle N \rangle \simeq 10^{-2}$ [Fig. 2 i): this is a non-equilibrium form of incompressibility. These regions follow the shape of the phase boundary [panel g)] predicted for a $T = 0$ equilibrium 1D system, that we obtained by means of matrix-product-states (MPS) simulations with $L = 200$ sites (see [40] for details on the approach): the agreement for the first lobe is excellent, while the deviations for the second lobe are due to a numerical cutoff in the maximum particle number per site $N_{\text{max}} = 3$ used in the steady-state calculation. Secondly, the insulating regions are separated by coherent regions with non-integer density, reminiscent of the equilibrium superfluid phase where excess particles/holes do not suffer from the photon blockade and can delocalize via tunneling: the condensed fraction is important and eventually reaches the maximal value $x_{\text{BEC}} = 1$ at high J , indicating a full coherence over the finite system.

While Fig. 2 focused on a limit case of parameters in order to validate the theoretical viability of our approach, Fig. 3 confirms its feasibility and the overall robustness of these features for state-of-the-art parameters in circuit-QED systems [34, 41]. The main consequence of the finite ratios Δ_{em}/U and $\Gamma_{\text{em}}^0/\Gamma_1$ is in fact a weak but appreciable value of particle number fluctuations $\Delta N \sim 0.13$, rather independent from tunneling.

Finite-size effects. Some of the discrepancies between the non-equilibrium steady-state and the thermodynamic limit prediction for the $T = 0$ state [dash dotted line in Fig. 2 i)] are likely to be finite-size effects, as they are also visible in the finite size equilibrium plot of Fig. 2 g): the insulating regions do not close completely to form lobes but end with a stripe, x_{BEC} is not exactly zero even at very weak J , and all observables present a smooth crossover for increasing tunneling in-

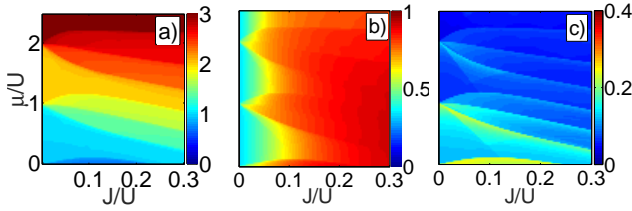


FIG. 3: Steady-state properties for $L = 3$, for state-of-the-art parameters in circuit QED. Panel a): average photon number per site n_{ph} . Panel b): condensed fraction x_{BEC} . Panel c): relative fluctuations of the total particle number ΔN . Parameters inspired from circuit-QED systems [34, 41]: $U = 2\pi \times 200\text{MHz}$, $\Delta_{\text{em}} = 2\pi \times 0.5\text{MHz}$, $\Gamma_{\text{em}}^0 = 2\pi \times 30\text{kHz}$, $\Gamma_1 = 2\pi \times 1\text{kHz}$, $N_{\text{max}} = 6$

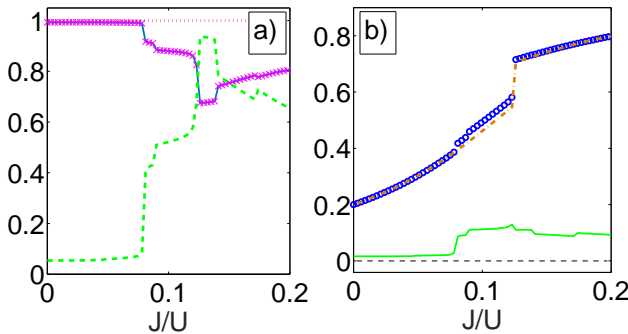


FIG. 4: Steady-state statistical properties for $L = 5$ at fixed $\mu = 0.55 U$. Panel a): fidelity \mathcal{F} between the steady state and the Hamiltonian ground state (blue solid line), occupancy π_0 of the most populated state $|\psi\rangle_+$ (purple crosses), overlap $|\langle\psi_+|GS\rangle|^2$ between the ground state and the most populated state (red dot line), entropy S (green dash line). Panel b): number fluctuations ΔN (green solid line) and condensed fraction (blue circles), compared to the $T = 0$ equilibrium value (orange dash-dot line). Same parameters as in Fig. 2.

stead of a sharp transition. As we can see in Fig. 2 [b), d), f)], for increasing system sizes, both the width of the stripes and the condensed fraction inside the insulating region decreases as $1/L$. One could be tempted to assume that the connection with $T = 0$ predictions is maintained for an infinite system size, leading to the emergence of Mott lobes surrounded by a superfluid (and possibly also Bose-condensed depending on the dimensionality) phase. However, as we are now going to discuss, specifically non-equilibrium features give rise to a richer phenomenology.

Non-equilibrium features. While in most parts of the insulating region the steady state presents an almost vanish entropy $S = \langle \ln(\rho_\infty) \rangle$ [Fig. 2 j)] and can thus be well approximated by a pure quantum state (as for a $T = 0$ equilibrium state), this is not the case in some regimes of parameters (especially in the coherent regime) where $S > 0$. To quantitatively characterize this behaviour, we looked at the fidelity $\mathcal{F} = \langle \text{GS} | \rho_\infty | \text{GS} \rangle$ between the steady state ρ_∞ and the Hamiltonian ground state $|\text{GS}\rangle$, and at the steady-state oc-

cupancy π_0 of the most populated state $|\psi_+\rangle$ [46].

Most strikingly, this phenomenon takes the form of a discontinuous transition in entropy [Fig. 4a)] from a 99% pure quantum state toward a statistical mixture above some critical J_c , located within an insulating region at a small but finite distance from the equilibrium transition line [Fig. 2 j)]. Note that this jump is present even for finite sizes L , and just gets smoother for the state-of-the-art parameters of Fig. 3. In the pure region $\mathcal{F} = \pi_0 \simeq 0.993$ are close to unity, indicating that ρ_∞ can be well approximated by the pure state $|\text{GS}\rangle \langle \text{GS}|$ (not the case in the entropic region). In both regions, $|\langle\psi_+|GS\rangle|^2 = 1$ (within machine precision), \mathcal{F} and π_0 take identical values, so the most populated state $|\psi_+\rangle$ is precisely equal to the Hamiltonian ground state at any value of J (at least for the precise value of μ in Fig. 4 a)). Looking at the observable x_{BEC} [Fig. 4 b)], the pure (resp. entropic) region is characterized by negligible (resp. small) deviations from equilibrium, and very weak fluctuations $\Delta N \simeq 0.016$ (resp. non-zero $\Delta N \simeq 0.13$).

This effect can be physically understood in terms of the departure from a true detailed balance relation: the emission spectrum is in fact not exponential in the frequency but rather decays with a power law above ω_+ and saturates at the value Γ_{em}^0 below ω_+ . For $J > J_c$, some dynamically non-equilibrium processes open up, through which the system can escape from the ground state. Eventually it ends up trapped for a while in slightly excited states with few more photons (more details in [37]). Whether this unexpected feature will affect the phase diagram in the thermodynamic limit in a dramatic manner (e.g., by destabilizing equilibrium phases [42] and/or giving rise to novel exotic ones [18–20]) is a complex question that goes beyond the scope of this work, and will be studied separately [39].

Conclusions. We have introduced a novel pumping scheme allowing to cool down strongly interacting driven-dissipative photonic systems toward incompressible states. Starting from a dissipative Bose-Hubbard model and using state-of-the-art parameters in circuit QED, we have demonstrated the feasibility of stabilizing Mott-Insulator-like states which are robust against tunneling and losses, and can be reshaped into coherent superfluid-like states for a suitable variation of parameters. Specifically non-equilibrium features due to deviations from detailed balance are finally illustrated. From a broad perspective, our study puts forward a promising protocol for photonic quantum simulations.

Acknowledgements. Discussions with Atac Imamoglu, Jonathan Simon, Jamir Marino and Leonardo Mazza are warmly acknowledged. JL and IC are supported by the EU-FET Proactive grant AQuS, Project No. 640800, and by the Autonomous Province of Trento, partially through the project “On silicon chip quantum optics for quantum computing and secure communications” (“SiQuro”). AB, FS and CC acknowledge support from ERC (via Consolidator Grant CORPHO No. 616233). RF acknowledges support from EU-QUIC. AB, CC, DR, and IC acknowledge the Kavli Institute for Theoretical Physics, University of California, Santa Bar-

bara (USA) for the hospitality and support during the early stage of this work.

* Electronic address: jose.lebreuilly@unitn.it

[1] I. Carusotto and C. Ciuti, *Rev. Mod. Phys.* **85**, 299 (2013).

[2] M. J. Hartmann, *J. Opt.* **18**, 104005 (2016).

[3] C. Noh and D. G. Angelakis, *Rep. Prog. Phys.* **80**, 016401 (2017).

[4] A. Imamoğlu, H. Schmidt, G. Woods, and M. Deutsch, *Phys. Rev. Lett.* **79**, 1467 (1997).

[5] K. M. Birnbaum, A. Boca, R. Miller, A. D. Boozer, T. E. Northup, and H. J. Kimble, *Nature* **436**, 87 (2005).

[6] C. Lang, D. Bozyigit, C. Eichler, L. Steffen, J. M. Fink, A. A. Abdumalikov, Jr., M. Baur, S. Filipp, M. P. da Silva, A. Blais, and A. Wallraff, *Phys. Rev. Lett.* **106**, 243601 (2011).

[7] A. Faraon, I. Fushman, D. Englund, N. Stoltz, P. Petroff, and J. Vuckovic, *Nat. Phys.* **4** 859 (2008).

[8] A. Reinhard, T. Volz, M. Winger, A. Badolato, K. J. Hennessy, E. L. Hu, and A. Imamoğlu, *Nature Photonics* **6**, 93 (2012).

[9] J. D. Pritchard, D. Maxwell, A. Gauguet, K. J. Weatherill, M. P. A. Jones, and C. S. Adams, *Phys. Rev. Lett.* **105**, 193603 (2010).

[10] T. Peyronel, O. Firstenberg, Q.-Y. Liang, S. Hofferberth, A. V. Gorshkov, T. Pohl, M. D. Lukin, and V. Vuletić, *Nature* **488**, 5760 (2012).

[11] D. L. Underwood, W. E. Shanks, J. Koch, and A. A. Houck, *Phys. Rev. A* **86**, 023837 (2012).

[12] M. Hafezi, S. Mittal, J. Fan, A. Migdall, and J. Taylor, *Nat. Photon.* **7**, 1001 (2013).

[13] D. Tanese, E. Gurevich, F. Baboux, T. Jacqmin, A. Lemaître, E. Galopin, I. Sagnes, A. Amo, J. Bloch, and E. Akkermans, *Phys. Rev. Lett.* **112**, 146404 (2014).

[14] A. Amo, J. Lefrère, S. Pigeon, C. Adrados, C. Ciuti, I. Carusotto, R. Houdré, E. Giacobino, and A. Bramati, *Nature Physics* **5**, 805 (2009).

[15] C. W. Lai, N. Y. Kim, S. Utsunomiya, G. Roumpos, H. Deng, M. D. Fraser, T. Byrnes, P. Recher, N. Kumada, T. Fujisawa, and Y. Yamamoto, *Nature* **450**, 529 (2007).

[16] T. Jacqmin, I. Carusotto, I. Sagnes, M. Abbarchi, D.D. Solnyshkov, G. Malpuech, E. Galopin, A. Lematre, J. Bloch, and A. Amo, *Phys. Rev. Lett.* **112**, 116402 (2014).

[17] M. Fitzpatrick, N. M. Sundaresan, A. C. Y. Li, J. Koch, and A. A. Houck, *Phys. Rev. X* **7**, 011016 (2017).

[18] J. Jin, D. Rossini, R. Fazio, M. Leib, and M. J. Hartmann, *Phys. Rev. Lett.* **110**, 163605 (2013).

[19] J. Jin, D. Rossini, M. Leib, M. J. Hartmann, and Rosario Fazio, *Phys. Rev. A* **90**, 023827 (2014).

[20] J. Jin, A. Biella, O. Viyuela, L. Mazza, J. Keeling, R. Fazio, and D. Rossini, *Phys. Rev. X* **6**, 031011 (2016).

[21] R. B. Laughlin, *Phys. Rev. Lett.* **50**, 1395 (1983).

[22] E. Kapit, M. Hafezi, and S. H. Simon, *Phys. Rev. X* **4**, 031039 (2014).

[23] M. P. A. Fisher, P. B. Weichman, G. Grinstein, and D. S. Fisher, *Phys. Rev. B* **40**, 546 (1989).

[24] I. B. Spielman, W. D. Phillips, and J. V. Porto, *Phys. Rev. Lett.* **98**, 080404 (2007).

[25] M. J. Hartmann, F. G. S. L. Brandão, and M. B. Plenio, *Nat. Phys.* **2**, 849 (2006).

[26] D. G. Angelakis, M. F. Santos, and S. Bose, *Phys. Rev. A* **76**, 031805 (2007).

[27] A. D. Greentree, C. Tahan, J. H. Cole, and L. C. L. Hollenberg, *Nat. Phys.* **2**, 856 (2006).

[28] I. Carusotto, D. Gerace, H. E. Tureci, S. De Liberato, C. Ciuti, and A. Imamoğlu, *Phys. Rev. Lett.* **103**, 033601 (2009).

[29] A. Tomadin and R. Fazio, *J. Opt. Soc. Am. B* **27**, A130 (2010).

[30] L. Henriet, Z. Ristivojevic, P. P. Orth, and K. Le Hur, *Phys. Rev. A* **90**, 023820 (2014).

[31] M. Biondi, G. Blatter, H. E. Türeci, and S. Schmidt, arXiv:1611.00697.

[32] J. Lebreuilly, I. Carusotto, and M. Wouters, *C. R. Phys.* **17**, 836 (2016), (preprint on arxiv arXiv:1502.04016).

[33] M. Hafezi, P. Adhikari, and J. M. Taylor, *Phys. Rev. B* **92**, 174305 (2015).

[34] R. Ma, C. Owens, A. Houck, D. I. Schuster, and J. Simon, arXiv:1701.04544.

[35] L. Pitaevskii and S. Stringari, *Bose-Einstein Condensation* (Oxford University Press, 2003).

[36] H.-P. Breuer and F. Petruccione, *The theory of open quantum systems* (Clarendon Press, Oxford, 2006).

[37] See Supplemental Material (next page) for analytical expressions of the emission power spectrum (as well as the memory kernel and the Lamb shift), for a sketch of the derivation of the photonic master equation (S19), and details on non-equilibrium features of the steady state.

[38] N. D. Mermin and H. Wagner, *Phys. Rev. Lett.* **17**, 1133 (1966).

[39] A. Biella, F. Storme, J. Lebreuilly, D. Rossini, I. Carusotto, R. Fazio, C. Ciuti, in preparation.

[40] T. D. Kühner, S. R. White, and H. Monien, *Phys. Rev. B* **61**, 12474 (2000).

[41] C. Rigetti, J. M. Gambetta, S. Poletto, B. L. T. Plourde, J. M. Chow, A. D. Córcoles, J. A. Smolin, S. T. Merkel, J. R. Rozen, G. A. Keefe, M. B. Rothwell, M. B. Ketchen, and M. Steffen, *Phys. Rev. B* **86**, 100506(R) (2012).

[42] E. Altman, L. M. Sieberer, L. Chen, S. Diehl, and J. Toner, *Phys. Rev. X* **5**, 011017 (2015).

[43] The secular approximation involves discarding fast oscillating terms in the master equation: for very weak dissipation and in absence of relevant degeneracies of the photonic Hamiltonian, the diagonal terms of the density matrix in the Hamiltonian eigenbasis are not coupled to off-diagonal terms, and the latter can be neglected when computing the steady state.

[44] We checked this numerically for 1D chains with $L = 3, 4$ and 5 .

[45] Due to numerical complexity of open quantum many-body problems and the lack of defined methods for tackling non-Markovian ones, we are severely limited in the system sizes we can simulate.

[46] To avoid possible artifacts such as the preferential choice of the steady-state eigenbasis, all these physical quantities were computed for $L = 5$ by exact steady-state calculation without using the secular approximation.

Supplemental Material

ANALYTICAL EXPRESSION FOR THE EMISSION SPECTRUM SHAPE

Here we give the precise analytical expressions for the emission spectrum $\mathcal{S}_{\text{em}}(\omega) = \Gamma_{\text{em}}^0 s_{\text{em}}(\omega)$. It is defined as the convolution product between the square-shape function $s_{\text{square}}(\omega) = \theta(\omega - \omega_-) \theta(\omega_+ - \omega)$ and a Lorentzian function of width Δ_{em} : $s_{\text{em}} = A(\omega)/A \left(\frac{\omega_+ + \omega_-}{2} \right)$ where

$$\begin{aligned} A(\omega) &= \int_{\omega_-}^{\omega_+} d\omega' \frac{\Delta_{\text{em}}/2}{(\omega - \omega')^2 + (\Delta_{\text{em}}/2)^2} \\ &= \left[\arctan \left(\frac{\omega_+ - \omega}{\Delta_{\text{em}}/2} \right) - \arctan \left(\frac{\omega_- - \omega}{\Delta_{\text{em}}/2} \right) \right]. \end{aligned} \quad (\text{S1})$$

With this expression it is possible to compute the emission memory kernel

$$\Gamma_{\text{em}}(\tau) = \frac{i\Gamma_{\text{em}}^0}{4} \frac{\theta(\tau)}{\tau} \frac{e^{(-i\omega_+ - \Delta_{\text{em}}/2)\tau} - e^{(-i\omega_- - \Delta_{\text{em}}/2)\tau}}{\arctan \left(\frac{\omega_+ - \omega_-}{\Delta_{\text{em}}} \right)}, \quad (\text{S2})$$

as well as its Fourier transform

$$\Gamma_{\text{em}}(\omega) = \frac{\Gamma_{\text{em}}^0}{2} s_{\text{em}}(\omega) - i\delta_{\text{lamb}}(\omega), \quad (\text{S3})$$

where the frequency-dependent lamb-shift is given by

$$\delta_{\text{lamb}}(\omega) = \frac{\Gamma_{\text{em}}^0}{2} \frac{\log \left(\frac{(\omega_+ - \omega)^2 + (\Delta_{\text{em}}/2)^2}{(\omega_+ - \omega_-)^2 + (\Delta_{\text{em}}/2)^2} \right)}{4 \arctan \left(\frac{\omega_+ - \omega_-}{\Delta_{\text{em}}} \right)}. \quad (\text{S4})$$

When a transition frequency come close to the upper edge $\omega \simeq \omega_+$, the logarithm contribution can lead to an increase of the Lamb shift with respect to the power spectrum $S_{\text{em}}(\omega) \sim \Gamma_{\text{em}}^0$. However the logarithm diverges very slowly close to its singularities, and for our range of parameters (in the weakly dissipative regime) we have that the Lamb shift is at most $\delta_{\text{lamb}}^{\text{max}} \sim 10\Gamma_{\text{em}}^0 \ll \Delta_{\text{em}}, U \dots$ and can thus be safely neglected.

DERIVATION OF THE PROJECTED PHOTONIC MASTER EQUATION STARTING FROM A MICROSCOPIC MODEL

In this section, we give more details on the derivation of the photonic master equation introduced in the beginning of this letter, starting from the microscopic model proposed to engineer the pump. We focus for simplicity on the case of one cavity with a single embedded two-level atom. Starting from the full atom-cavity master equation, we show how for a sufficiently small atom-cavity coupling Ω_R the atomic degrees of freedom can be eliminated. The frequency-dependence of the atomic amplification is then accounted for as a modified Lindblad term. Our treatment is based on the discussion in the textbook [S1].

General formalism

We consider a quantum system which undergoes dissipative processes. As it is not isolated, its state can not be described by a wave function but by a density matrix ρ evolving according to the master equation:

$$\partial_t \rho = \mathcal{L}(\rho(t)), \quad (\text{S5})$$

where \mathcal{L} is some linear “super-operator” acting on the space of density matrices. Given an arbitrary initial density matrix $\rho(t_0)$, the density matrix ρ at generic time t is equal to $\rho(t) = e^{\mathcal{L}(t-t_0)} \rho(t_0)$.

Now we are only interested in some part of the density matrix, which can represent some subsystem. This can be described by a projection operation on the density matrix $\mathcal{P}\rho$. We call $\mathcal{Q} = 1 - \mathcal{P}$ the complementary projector. We decompose the Lindblad operator \mathcal{L} in two parts \mathcal{L}_0 and $\delta\mathcal{L}$ such that:

$$\begin{cases} \mathcal{L} = \mathcal{L}_0 + \delta\mathcal{L} \\ \mathcal{P}\mathcal{L}_0\mathcal{Q} = \mathcal{Q}\mathcal{L}_0\mathcal{P} = 0 \\ \mathcal{P}\delta\mathcal{L}\mathcal{P} = 0. \end{cases} \quad (\text{S6})$$

Such a decomposition is always possible.

Then we define a generalised interaction picture for the density matrix and for generic superoperators \mathcal{A} with respect to the evolution described by the free \mathcal{L}_0 and the initial time t_0 :

$$\begin{cases} \hat{\rho}(t) = e^{-\mathcal{L}_0(t-t_0)} \rho(t) \\ \hat{\mathcal{A}}(t) = e^{-\mathcal{L}_0(t-t_0)} \mathcal{A} e^{\mathcal{L}_0(t-t_0)}. \end{cases} \quad (\text{S7})$$

As discussed in [S1], we can get an exact closed master equation for the projected density matrix in the interaction picture

$$\partial_t \mathcal{P}\hat{\rho}(t) = \int_{t_0}^t dt' \Sigma(t, t') \mathcal{P}\hat{\rho}(t'), \quad (\text{S8})$$

which translates to

$$\partial_t \mathcal{P}\rho(t) = \mathcal{L}_0(\rho(t)) + \int_{t_0}^t dt' \tilde{\Sigma}(t-t') \mathcal{P}\rho(t') \quad (\text{S9})$$

in the Schrodinger picture. In the interaction picture, the self energy operator Σ is defined as:

$$\begin{aligned} \Sigma(t, t') &= \sum_{n=2}^{\infty} \int_{t'}^t \int_{t'}^{t_1} \dots \int_{t'}^{t_{n-1}} dt_1 \dots dt_n \\ &\quad \mathcal{P}\delta\hat{\mathcal{L}}(t)\mathcal{Q}\delta\hat{\mathcal{L}}(t_1)\mathcal{Q}\delta\hat{\mathcal{L}}(t_2)\dots\mathcal{Q}\delta\hat{\mathcal{L}}(t_n)\mathcal{Q}\delta\hat{\mathcal{L}}(t')\mathcal{P} \end{aligned} \quad (\text{S10})$$

and results from the coherent sum over the processes leaving from \mathcal{P} , remaining in \mathcal{Q} and then coming back finally to \mathcal{P} . In the Schrodinger representation, we have:

$$\tilde{\Sigma}(t-t') = e^{\mathcal{L}_0(t-t_0)} \Sigma(t, t') e^{-\mathcal{L}_0(t'-t_0)} = \Sigma(0, t'-t) e^{\mathcal{L}_0(t-t')}. \quad (\text{S11})$$

We call $\tau_c = 1/\Delta\omega$ the characteristic decay time / inverse linewidth for the self energy, which corresponds in general to the correlation time of the bath, and we estimate the rate of dissipative processes as $\Gamma \sim \max_\omega |\tilde{\Sigma}(\omega)|$. We put ourselves in the regimes in which, with respect to these dissipative processes, the bath has a short memory, ie $\Gamma \ll \Delta\omega$. In that regime the density matrix in the interaction picture is almost constant over that time τ_c . Furthermore, if $t - t_0 \gg \tau_c$ then the integral in eq (S8) can be extended from $-\infty$ to t . From this equation and from (S8), by going back in the Schrodinger picture we get an equation of evolution for the density matrix which is local in time:

$$\partial_t \mathcal{P}\hat{\rho}(t) = \left[\mathcal{L}_0 + \int_0^\infty d\tau \Sigma(0, -\tau) \right] \mathcal{P}\rho(t) = \mathcal{L}_{\text{eff}} \mathcal{P}\rho(t), \quad (\text{S12})$$

with

$$\mathcal{L}_{\text{eff}} = \mathcal{L}_0 + \int_0^\infty d\tau \Sigma(0, -\tau). \quad (\text{S13})$$

It is worth stressing that while the bath is Markovian with respect to dissipative processes induced by the perturbation $\int_0^\infty d\tau \Sigma(0, -\tau)$, no Markovian approximation has been made with respect to the dynamics due to \mathcal{L}_0 , which can still be fast. For the specific system under consideration in this work, this means that the emission rate Γ_{em} has to be slow with respect to the gain bandwidth set by the atomic pumping rate Γ_p , which is the case in the weak coupling limit $\sqrt{N_{\text{at}}} \Omega_R \ll \Gamma_p$. However no restriction is to be imposed on the parameters U , J and $\omega_{\text{cav}} - \omega_{\text{at}}$ of the Hamiltonian, which can be arbitrarily large. This means that the physics can be strongly non-Markovian with respect to the Hamiltonian photonic dynamics.

Application to the array of cavities

Preliminary calculations

With the notation of our {atoms+cavity modes} proposal of implementation, we choose the projectors in the form:

$$\mathcal{P}\rho = \left| \{e_i^{(n)}\} \right\rangle \left\langle \{e_i^{(n)}\} \right| \otimes \text{Tr}_{\text{at}}(\rho), \quad (\text{S14})$$

where we have performed a partial trace over the embedded atoms in all cavities, and then make the tensor product of the density matrix and the atomic density matrix with all atoms in the excited state. We chose this particular projector because in the weak atom-cavity coupling regime, we expect atoms to be repumped almost immediately after having emitted a photon in the cavity array, and thus to be most of the time in the excited state. Moreover this projection operation gives us direct access to the photonic density matrix, and thus we do not lose any information on photonic statistics. Applying the method sketched in the previous section, and restricting ourselves to

the single atom-single cavity configuration, we derive the following photonic master equation (see [S2] for the details of the derivation):

$$\begin{aligned} \partial_t \rho = & -i [H_{\text{ph}}, \rho_{\text{ph}}] + \frac{\Gamma_1}{2} [2a\rho a^\dagger - a^\dagger a\rho - \rho a^\dagger a] \\ & + \frac{2\Omega_R^2}{\Gamma_p} [\tilde{a}^\dagger \rho a + a^\dagger \rho \tilde{a} - a \tilde{a}^\dagger \rho - \rho \tilde{a} a^\dagger], \end{aligned} \quad (\text{S15})$$

with

$$\begin{cases} \tilde{a} = \frac{\Gamma_p}{2} \int_0^\infty d\tau e^{(-i\omega_{\text{at}} - \Gamma_p/2)\tau} a(-\tau), \\ \tilde{a}^\dagger = \frac{\Gamma_p}{2} \int_0^\infty d\tau e^{(i\omega_{\text{at}} - \Gamma_p/2)\tau} a^\dagger(-\tau) = [\tilde{a}]^\dagger, \end{cases} \quad (\text{S16})$$

where $a(-\tau)$ means the photonic annihilation operator in the photonic Hamiltonian interaction picture.

If $|f\rangle$ and $|f'\rangle$ are two eigenstates of the photonic Hamiltonian with a photon number difference of one, we see that the matrix elements of the modified annihilation and creation operators \tilde{a} and \tilde{a}^\dagger involved in the emission process are:

$$\begin{cases} \langle f | \tilde{a} | f' \rangle = \frac{\Gamma_p/2}{-i(\omega_{f'} - \omega_{\text{at}}) + \Gamma_p/2} \langle f | a | f' \rangle \\ \langle f' | \tilde{a}^\dagger | f \rangle = \frac{\Gamma_p/2}{i(\omega_{f'} - \omega_{\text{at}}) + \Gamma_p/2} \langle f' | a^\dagger | f \rangle. \end{cases} \quad (\text{S17})$$

The non-Markovianity comes from the energy-dependence of the prefactors.

For this simple configuration and with the notations of the main text [Eq. (4)], we have thus that $\Gamma_{\text{em}}(\tau) = 2\Omega_R^2 \theta(\tau) e^{(-i\omega_{\text{at}} - \Gamma_p/2)\tau}$ and $\Gamma_{\text{em}}(\omega) = \frac{\Gamma_{\text{em}}^{\text{at}}}{2} \frac{\Gamma_p/2}{-i(\omega - \omega_{\text{at}}) + \Gamma_p/2}$, where $\Gamma_{\text{em}}^{\text{at}} = \frac{4\Omega_R^2}{\Gamma_p}$ is the emission rate of a single atom at the top of the Lorentzian.

Master equation for many cavities and many atoms

For several cavities and a large number N_{at} of atoms per cavity (modeled by a continuum of bare-frequencies with the distribution $\mathcal{D}(\omega)$), the reasoning is exactly the same: each atom brings its own infinitesimal contribute to the total frequency-dependent emission, and by making the continuous sum of all of these terms we get the multicavity master equation

$$\begin{aligned} \partial_t \rho = & -i [H_{\text{ph}}, \rho(t)] + \mathcal{L}_1(\rho(t)) + \\ & \frac{\Gamma_{\text{em}}^0}{2} \sum_{i=1}^L \left[\tilde{a}_i^\dagger \rho a_i + a_i^\dagger \rho \tilde{a}_i - a_i \tilde{a}_i^\dagger \rho - \rho \tilde{a}_i a_i^\dagger \right], \end{aligned} \quad (\text{S18})$$

where

$$\frac{\Gamma_{\text{em}}^0}{2} \tilde{a}_i = \int_0^\infty d\tau \Gamma_{\text{em}}(\tau) a_i(-\tau), \quad \tilde{a}_i^\dagger = [\tilde{a}_i]^\dagger \quad (\text{S19})$$

is the modified annihilation operator,

$$\Gamma_{\text{em}}(\tau) = \Gamma_{\text{em}}^{\text{at}} \theta(\tau) \int d\tilde{\omega} \mathcal{D}(\tilde{\omega}) e^{-(i\tilde{\omega} + \Gamma_p/2)\tau} \quad (\text{S20})$$

$$= \theta(\tau) \int \frac{d\omega}{2\pi} \mathcal{S}_{\text{em}}(\omega) e^{-i\omega\tau} \quad (\text{S21})$$

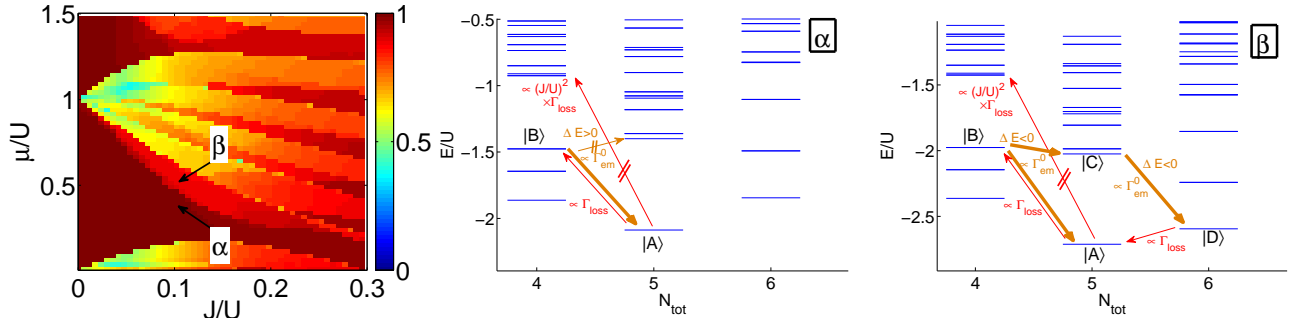


FIG. S1: Left panel: Occupancy π_0 of the most populated quantum state at steady state for a 5 sites system. Central (resp. right) panel: spectrum of H_{eff} at the values $J/U = 0.1$ and $\mu/U = 0.38$ (resp. $\mu/U = 0.55$) indicated by the point $[\alpha]$ (resp. $[\beta]$) in the left panel. Parameters used: $\Gamma_1/\Gamma_{\text{em}} = 10^{-3}$, $U/\Delta_{\text{em}} = 10^6$, $\Gamma_{\text{em}}^0/\Delta_{\text{em}} = 10^{-2}$, $\omega_+ = 0$, $\omega_-/\Delta_{\text{em}} = -4 \cdot 10^7$.

is the causal autocorrelation for photonic emission,

$$\mathcal{S}_{\text{em}}(\omega) = \Gamma_{\text{em}}^{\text{at}} \int d\tilde{\omega} \mathcal{D}(\tilde{\omega}) \frac{(\Gamma_p/2)^2}{(\omega - \tilde{\omega})^2 + (\Gamma_p/2)^2} \quad (\text{S22})$$

is the photonic emission power spectrum and $\Gamma_{\text{em}}^{\text{at}}$ has been defined in the previous paragraph. $\mathcal{S}_{\text{em}}(\omega)$ is the convolution product of a Lorentzian which represents the broadening of each atom due to the pumping, and the spectral distribution $\mathcal{D}(\omega)$ of the atomic bare frequencies in absence of pumping. In our case, the distribution is square-shape $\mathcal{D}^{\text{square}}(\omega) = \frac{N_{\text{at}}}{\omega_+ - \omega_-} \theta(\omega - \omega_-) \theta(\omega_+ - \omega)$, so we obtain the form for the emission power spectrum:

$$\mathcal{S}_{\text{em}}^{\text{square}}(\omega) = \Gamma_{\text{em}}^{\text{at}} \frac{N_{\text{at}}}{\omega_+ - \omega_-} \int_{\omega_-}^{\omega_+} d\tilde{\omega} \frac{(\Delta_{\text{em}}/2)^2}{(\omega - \tilde{\omega})^2 + (\Delta_{\text{em}}/2)^2}, \quad (\text{S23})$$

with $\Delta_{\text{em}} = \Gamma_p$. The maximum power spectrum obtained at the middle between the two cutoffs is then

$$\begin{aligned} \Gamma_{\text{em}}^0 &= \mathcal{S}_{\text{em}}^{\text{square}} \left(\frac{\omega_+ + \omega_-}{2} \right) \\ &= \frac{2\pi N_{\text{at}} \Omega_R^2}{\omega_+ - \omega_-} \quad \text{for } \Delta_{\text{em}} \ll \omega_+ - \omega_- \end{aligned} \quad (\text{S24})$$

DISCREPANCIES BETWEEN THE STEADY STATE AND THE ZERO TEMPERATURE STATE

In this section we discuss more extensively the presence in some regions of the phase diagram of differences between the steady state and the zero temperature state, and, in particular, the presence of a finite entropy: the steady state is not exactly a pure quantum state, but rather slightly mixes the Hamiltonian ground state with some other state with more particles. Below we will focus our discussion on 5 sites simulations. The occupancy π_0 of the most populated quantum state of the density matrix at steady state is given in the left panel of Fig. SS1. We show in addition the spectrum of $H_{\text{eff}} = \sum_{i=1}^k \left[-\mu a_i^\dagger a_i + \frac{U}{2} a_i^\dagger a_i^\dagger a_i a_i \right] - J \sum_{\langle i,j \rangle} a_i^\dagger a_j$ at two points $[\alpha]$ and $[\beta]$ separated by a small variation of μ , with

respectively zero and non-zero entropy in the central and right panels.

From the analysis of the transition rates carried out in the Main Text one expects that the steady state occupation be concentrated in the ground state $|A\rangle$ of H_{eff} , i.e., a (weakly delocalized) Mott state with 1 photon per site. However looking at the spectrum of many-body quantum states for the choice of parameters indicated as $[\beta]$ (central panel of Fig. SS1), we note that, starting from $|A\rangle$ which contains $N_{\text{tot}} = 5$ photons in total, the system can lose one photon and arrive in an excited state $|B\rangle$ with $N_{\text{tot}} - 1$ photons. Then, the pump re-injects a new photon and brings the system into a quantum state $|C\rangle \neq |A\rangle$ with N_{tot} photons such that $E_C < E_B$. Since the spectrum has a square shape, the pump can bring the system toward both the ground state $|A\rangle$ and $|C\rangle$ with comparable efficiencies $\propto \Gamma_{\text{em}}^0$. There is one last state $|D\rangle$ with $N_{\text{tot}} + 1$ photons and energy E_D such that $E_D < E_C$ so the excited N_{tot} photon state $|C\rangle$ is unstable and gets quickly pumped toward $|D\rangle$ where it gets trapped for a while as no state with higher photon number and lower energy exists, until one photon gets lost and the system goes back to the ground state $|A\rangle$.

This mechanism explains why we observe, in the steady state, a photonic density slightly bigger than in the ground state with non-zero entropy. If the emission rate were exponentially dependent in the energy jump, the detailed balance condition would be verified, and the re-pumping process toward $|C\rangle$ would not be relevant since its efficiency will be dynamically overwhelmed by the process bringing the system back toward the ground state $|A\rangle$.

In contrast, for the choice of parameters indicated as $[\alpha]$, the ground state $|A\rangle$ is well isolated dynamically. Looking at the spectrum of many-body quantum states shown in the right panel of Fig. SS1), one sees that the only energetically authorized transition after losing one photon is to go back into the Mott ground state of N_{tot} photons. Of course there exist states with $N_{\text{tot}} - 1$ photons in an higher energy band which would allow the kind of processes described earlier. However those states correspond to highly excited doublet states and have an overlap $\propto J/U$ with the state $a_i |A\rangle$ in which we removed one photon to the ground state. The effective rate of

this process is thus of the order of $(J/U)^2\Gamma_1 \sim \Gamma_1/100$ and induces a negligible leak out of $|A\rangle$. As a consequence the steady state is almost pure, and corresponds very well to the Mott-like ground state.

We have numerically checked that similar exchanges in the energetic order of many-body levels are not restricted to the $L = 5$ case discussed here, but keep occurring also for larger system sizes. Their meaning in the thermodynamic limit will be subject of future investigations.

* Electronic address: jose.lebreuilly@unitn.it

[S1] H.-P. Breuer and F. Petruccione, *The theory of open quantum systems* (Clarendon Press, Oxford, 2006).

[S2] J. Lebreuilly, I. Carusotto, and M. Wouters, *C. R. Phys.* **17**, 836 (2016), (preprint on arxiv arXiv:1502.04016).